

## Lemon Juice Particulates. Some Effects of Juice Processing

Wayne Venolia\* and Shirley Peak<sup>1</sup>

Specimens of commercially processed lemon juice that represented extraction, finishing, pasteurization, and concentration were compared with some laboratory analogues. The basic experimental criteria were particle size and juice turbidity. Coulter Counter tubes with nominal aperture diameters of 50 and 200  $\mu\text{m}$  were calibrated with five latexes including one that was sized by light microscopy. Particle-size distribution results were analyzed with the help of numerical methods. Plots of differences between successive size distributions revealed how particle concentration changes were related to effective particle diameter and type of processing. Such plots showed that, over the range of effective diameters studied (0.8–55  $\mu\text{m}$ ), the larger particles in hand-reamed juice from one lot of fruit were particularly susceptible to loss during processing, while particles of similar size in commercially processed juice from another lot of fruit were comparatively resistant. Juice turbidity results and certain particle-size distribution characteristics appeared to be related.

Citrus juices contain particles that are referred to collectively as cloud. These particles play a role in establishing organoleptic properties that are directly related to juice quality. Previous work on the particulates of fresh, unpasteurized lemon juices and a commercial concentrate (Venolia et al., 1974) suggested that processing profoundly affects particle-size distributions. Because juice properties such as turbidity and particle settling rate are related to the particle-size distribution, it is of interest to explore the effects of processing upon the distributions. The present work combined advances in laboratory technique and data handling procedures with an investigation of particle-size distribution and turbidity in two groups of processed juice specimens.

### EXPERIMENTAL SECTION

**Aperture Calibration.** Coulter Counter apertures with nominal diameters of 50 and 200  $\mu\text{m}$  were recalibrated with the latexes used previously (Venolia et al., 1974) plus a new latex with a nominal diameter of 10.3  $\mu\text{m}$  (Duke Standards Co., Palo Alto, Calif.). The new latex was sized by two workers who randomly selected and measured 200 particles each, using a light microscope with an eyepiece micrometer that was calibrated with a Bausch and Lomb 31-16-99 stage micrometer. The final item in Table I is the mean diameter of the 400 particles. The other values in the last column were obtained by application of the new instrument constant (the expression that defines the instrument constant was given in Venolia et al., 1974) for the 50- $\mu\text{m}$  aperture to the experimental half-count thresholds. Although the instrument constant for the 200- $\mu\text{m}$  aperture was based solely upon the new latex, that for the 50- $\mu\text{m}$  aperture was the mean of the values obtained with all of the latexes. Recalibration lowered the instrument constant 1.9 and 7.3% for the 50- and 200- $\mu\text{m}$  apertures, respectively.

**Description of Size Distributions.** Nonsubjective procedures for describing the salient features of a particle-size distribution facilitate analysis and comparison. The cubic curve-fitting routine used by Venolia et al. (1974) served well for many juices, but it was not readily

Table I. Aperture Recalibration<sup>a</sup>

Nominal diameter	Previous work <sup>b</sup>	Present work <sup>c</sup>
1.099	1.18	1.21
1.305	1.27	1.31
1.947	2.01	2.03
3.49	3.46	3.41
10.3		11.56

<sup>a</sup> Tabulated values are latex particle diameters in micrometers. <sup>b</sup> Original calibration results reported by Venolia et al. (1974). <sup>c</sup> See text for explanation of origin of new diameter data.

adapted to very narrow or multimodal distributions. After extensive testing of published curve-fitting methods (see, e.g., Carnahan et al. (1969) and Hahn and Shapiro (1967)) we decided that certain numerical procedures (Hildebrand, 1974) would permit the most suitable representation and analysis of our data. All curves were fitted with a first-degree, three-point smoothing procedure that was iterated once. Diameters representing the principal modes were located by numerical differentiation of the smoothed data. Because the size distributions varied considerably in skewness, a measure of central tendency was provided for comparison. This measure was selected to approximate the logarithmic mean diameter of the particles, and it was taken from the smoothed curve at half the maximum height. Both the modal and the logarithmic mean diameters are reported in Table II.

The widths of the particle-size distributions were also evaluated at half-height. Except for commercial concentrate, widths were estimated from the smoothed data by linear interpolation. The extrapolation required to define the width for plant concentrate was performed by assuming that particle concentration fell linearly from the 0.8- $\mu\text{m}$  point to the origin of coordinates; for present purposes, this approximation introduced negligible error.

**Scattering Strength.** Scattering strength, the ratio of turbidity index (defined in Venolia et al., 1974) to particle concentration, is provided to simplify comparison of the inherent light-scattering capabilities of the particle systems.

**Difference Distributions.** The data points in Figures 1 and 2 were used to obtain the difference distributions of Figures 3 and 4; e.g., curve A of Figure 3 represents the points of Figure 1C minus the points of Figure 1B. Curves were fitted by the procedure described earlier. Means of the deviations represented by Figures 3 and 4 are expressed as percentages in Table III.

Fruit and Vegetable Chemistry Laboratory, Agricultural Research Service, U.S. Department of Agriculture, Pasadena, California 91106.

<sup>1</sup>Present address: Biophysics Laboratory, Center for the Health Sciences, University of California, Los Angeles, California 90024.

Table II. Turbidity and Size Distribution Results

	Sample age, days	Particle concn, <sup>c</sup> mm <sup>3</sup> /g	Turbidity index	Diameter		Distribu- tion width, μm	Scatter- ing strength <sup>e</sup>
				Modal, μm	Log mean, <sup>d</sup> μm		
Plant processing <sup>a</sup>							
Control	0	10.7	4.3	3.18	3.23	8.49	0.4
Brown extracted	1-2 <sup>d</sup>	5.0	8.3	2.00	2.34	4.09	1.7
Paddle finished	1-2 <sup>d</sup>	5.6	10.9	2.15	2.12	3.34	1.9
Pasteurized	3	3.9	7.7	1.71	2.01	3.57	2.0
Concentrated <sup>f</sup>	6	2.6	5.1	1.24	1.11 <sup>h</sup>	1.64 <sup>h</sup>	2.0
Concentrated <sup>f</sup>	48	3.3	5.3	1.03	0.95 <sup>h</sup>	1.50 <sup>h</sup>	1.6
Laboratory processing <sup>b</sup>							
Control	0	6.5	6.3	2.23	2.34	4.24	1.0
Pasteurized	0	5.7	8.0	2.77	2.41	4.08	1.4
Concentrated <sup>g</sup>	3	3.7	5.4	1.75	2.01	2.93	1.5

<sup>a</sup> Placentia, Calif. lemons. <sup>b</sup> Upland, Calif. lemons. <sup>c</sup> Particles with less than 0.8 μm effective diameter not detected due to limited range of apparatus. <sup>d</sup> This is an approximation; see text. <sup>e</sup> Ratio of turbidity index to particle concentration; see text. <sup>f</sup> Tabulated data on single strength basis of 57.0 g/l. citric acid. <sup>g</sup> Tabulated data on single strength basis of 72.7 g/l. citric acid. <sup>h</sup> Small diameter limit by extrapolation, see text.

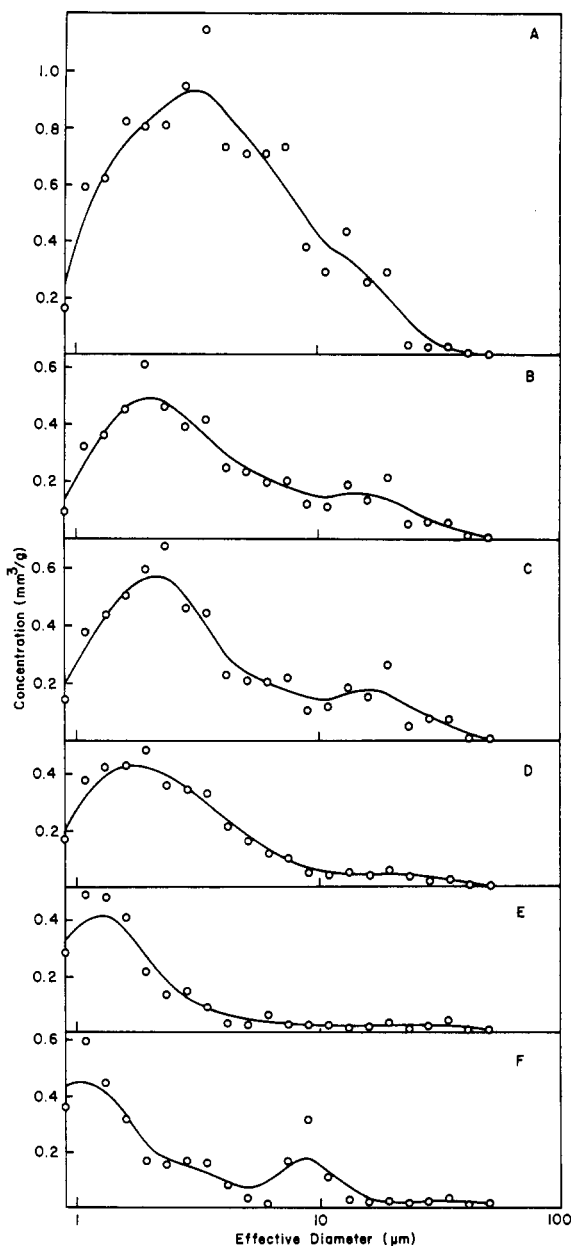


Figure 1. Particle size distributions pertaining to plant processing: (A) laboratory extracted; (B) plant extracted; (C) paddle finished; (D) pasteurized; (E) concentrated, 6 days storage; (F) concentrated, 48 days storage.

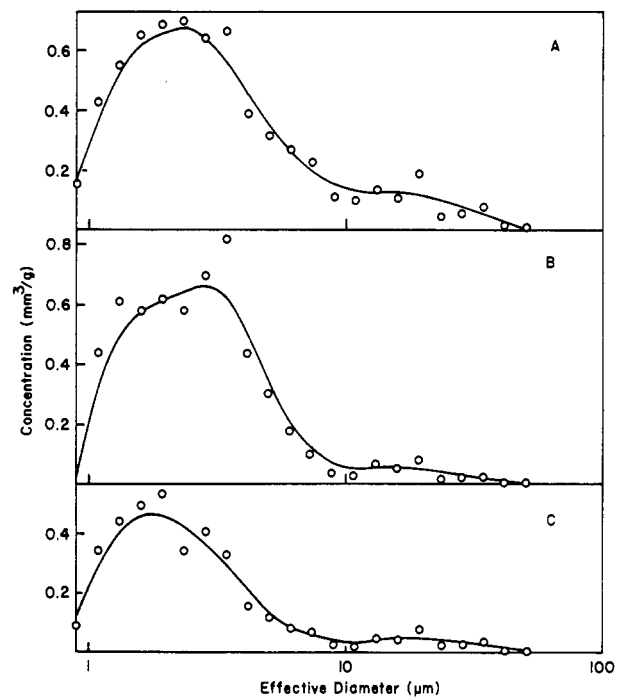


Figure 2. Particle size distributions from laboratory processing: (A) control; (B) pasteurized; (C) concentrated.

Table III. Comparison of Processing Stages

	Mean deviation % <sup>a</sup>
Plant processing	
Brown extracted vs. control	60.3
Paddle finished vs. Brown extracted	16.9
Pasteurized vs. paddle finished	37.9
Concentrated vs. pasteurized	50.9
Laboratory processing	
Pasteurized vs. control	36.1
Concentrated vs. control	51.7

<sup>a</sup> Derived from difference distributions; see text and Table II footnotes.

**Commercial Processing.** Commercial juice samples were acquired during a regular plant run. Except for the concentrate, sampling was timed so that each sample represented, as nearly as was practical, a single point in the plant stream. Since batch evaporation was used, the concentrate sample represented the whole plant run. The

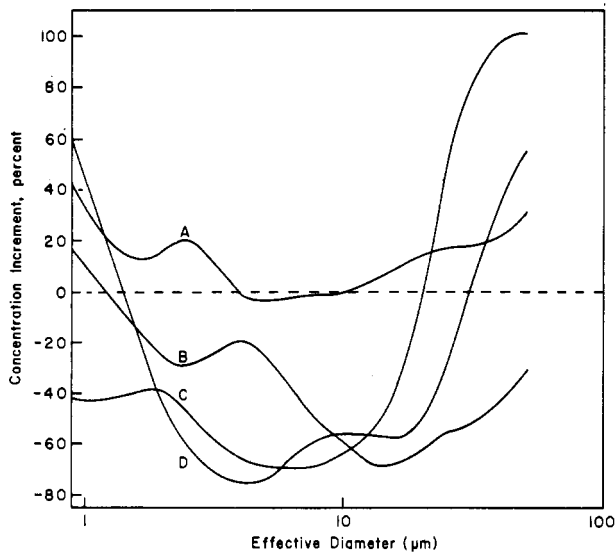


Figure 3. Difference distributions reflecting plant processing steps: (A) paddle finishing; (B) pasteurization; (C) extraction; (D) concentration.

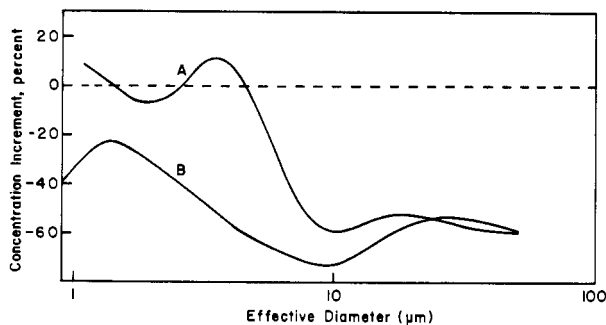


Figure 4. Difference distributions reflecting laboratory processing: (A) pasteurization; (B) concentration.

fresh juice control was prepared by established laboratory procedure (see next section) using 12 lemons randomly removed from the conveyor that fed the Brown extractors in the plant. Extractor effluent was paddle-finished and then rotary screened to remove pulp. Depulped juice was pasteurized for about 1 min at 90.6 °C and then fed to a Majonnier evaporator operating at 23.9 °C. The final citric acid value was 451.2 g/l.

Full-strength samples were quickly frit filtered at the plant and then iced and held near 0 °C until measurements were completed. A portion of the concentrate was examined as received; the rest was poured into glass vials, repeatedly backfilled with N<sub>2</sub>, sealed, and stored at about 0 °C.

Particle-size analysis was carried out in the order of sample acquisition. To minimize effects that could conceivably result from juice instability, the two samples representing extractor effluent and finisher effluent were examined in parallel: runs with the 50- $\mu$ m aperture were completed on one day and runs with the 200- $\mu$ m aperture on the next.

Note that while high hydraulic shear conditions frequently existed in the plant due to extraction, finishing, and pumping, there were no comparable shear conditions during laboratory processing.

**Laboratory Processing.** The straining of hand-reamed juice was facilitated by the replacement of cheese cloth with 6-mm glass spheres. A typical 50-ml juice sample was passed through  $33.2 \pm 0.1$  g of the spheres layered over the EC-porosity fritted glass disk. Other procedural details appear in Venolia et al. (1974). Hand-reamed juice was

pasteurized in a rotary evaporator (Buechi, Rotavapor R). A 250-ml flask held 100 ml of fresh juice that had been prepared for counting in the usual way (Venolia et al., 1974). The flask was rotated at full speed. Juice temperature was adjusted with baths held at 0 and 84 °C. The pasteurization sequence was: chilling, deaeration, back-filling with N<sub>2</sub>, heating, and chilling. Pilot measurements showed that the juice was in the pectinesterase deactivation range of 68–74 °C for 70 s. Overall processing time was 6.9 min.

The rotary evaporator was also used to prepare concentrate from the same type of feed juice. With a 36 °C bath and the maximum rotation rate, no bubbling was visible. The final citric acid value of 417.9 g/l. was attained in about 48 min with pumping at about 20 mm.

## RESULTS AND DISCUSSION

The numerical methods adopted for data treatment were sufficiently simple to be readily applied with a programmable calculator. Unpublished work with a variety of juice samples suggests that the precision of measurement was good. An example of precision attained is provided by the data of Venolia et al. (1974), where the triplicate measurements were made over an interval of about 2 months. In that work juice specimens from lots of 14 lemons gave standard deviations of 3.4 and 8.8% for modal diameter and distribution width, respectively. These estimates are somewhat larger than they would be if the data were corrected for fruit maturation effects. Returning to the present work note that the agreement between the first and last columns of Table I gives an indication of the size reliability that was attained. Table II summarizes results for juice turbidity and particle size distribution. Turbidity and size distribution are linked, at least in part, by the tendency of scattering efficiency to increase as particle size approaches the wavelength of light. In a complicated system such as lemon juice, quantitation of the relationship is not simple. In addition to the real complexity of the size distributions, there are effects due to differences in refractive index and particle morphology. Furthermore, many juice samples probably contain significant concentrations of light-scattering particles that are smaller than the present detection limit of 0.8  $\mu$ m; cf. the shapes of the size distribution curves in the region of small particle diameter. Despite these complications, Table II results are generally consistent with the hypothesis that reducing modal diameter tends to increase scattering strength. Two apparent contradictions of this hypothesis occurred. In the first instance, i.e., storage of plant concentrate, both scattering strength and modal diameter fell; we attributed this result to the largeness of the new particles (cf. Figures 1E and 1F). In the second instance, i.e., laboratory pasteurization, we attributed the rise in scattering strength that accompanied the rise in modal diameter to leftward skewing of the particle size distribution. Although other factors may have been significant (see later discussion), the augmented population of small scatterers implied by leftward skewing is expected, in general, to increase overall scattering strength.

Expression of the changes of particle concentration as percentages, as in Figures 3 and 4, simplifies the task of perceiving the effect of a processing stage upon a given size class of particles. Further data reduction, as in Table III, facilitates comparison of the overall ability of processing stages to reshape particle size distributions. The data in Table III are the means of the absolute values of particle concentration differences for a given processing stage.

Data for the plant control (Table II) are similar to the averages found in the laboratory for fresh, hand-reamed

lemon juice. Property changes in the plant processing series were often more striking than in the laboratory series. The yield of detectable particles from plant extraction was 53% below the yield for the control, and the deviation in the difference distribution was the largest that occurred (Table III, Brown-extracted vs. control). The distribution in Figure 3C shows at least 40% particle loss for all diameters below 13  $\mu\text{m}$  and as much as 70% in the vicinity of 7  $\mu\text{m}$ . These losses contrast with the significant gain of particles above 21  $\mu\text{m}$ . The foregoing changes are consistent with the emergence of the secondary peak with its mode at about 15.6  $\mu\text{m}$ ; cf. Figure 1B. The strong narrowing of particle size distribution and the reduction of particle diameters in the transition from laboratory to plant extraction correlate with the large increase in the turbidity indicators.

The net particulate concentration increase of about 12% in paddle finishing included particle loss between 4.0 and 10.4  $\mu\text{m}$ , roughly the same size range as for the region of heaviest loss by automatic extraction. This similarity suggests that the resistance of particles to disruption by shear depends to some extent upon the size of the particles. Paddle finishing significantly reduced distribution width with an attendant rise of the turbidity indicators; skewness shifted leftward.

Part of the loss of particle concentration detected at pasteurization may be due to depulping, but some of the loss probably represents the type of response found in laboratory processing; note the similarity of curve shape in Figures 3B and 4A. Aside from lowering particle concentration, the principal effect of pasteurization was to broaden the particle size distribution and skew it rightward. The growth of particle concentration below 1.2  $\mu\text{m}$  indicated in Figure 3B may be responsible for the slight increase of scattering strength found at this stage.

The somewhat arbitrary reference level of 57.0 g/l. citric acid for plant concentrate makes the tabulated particle concentration and turbidity equally arbitrary. The reference level, however, does not influence the other data in Table II where the diameter values and distribution width of concentrate decreased while the scattering strength was unaltered. Concentration in the plant and in the laboratory produced comparable, large deviations in the difference distributions. Particle concentration loss was greatest at about 4  $\mu\text{m}$  and was large throughout most of the range 1.4–31.5  $\mu\text{m}$ ; outside these limits particle concentration increased.

The particle size distribution of plant concentrate was not stable. After 48 days of storage, net particle concentration increased, diameter and width values decreased, and, most strikingly, there was growth of particles having a modal diameter of about 9  $\mu\text{m}$ ; cf. Figure 1F.

The log mean diameter and distribution width derived from the Figure 2A data are especially small for fresh, hand-reamed juice, and the turbidity results are particularly high. These departures from possible norms may reflect the comparative freshness of the fruit whose yellowing had been accelerated by ethylene treatment. Laboratory pasteurization of this sample caused an overall particle concentration loss of only 12%; nevertheless, there were profound changes. All particle sizes above 4.5  $\mu\text{m}$  experienced loss (as much as 60% for some sizes; cf. Figure 4A). Turbidity indicators rose sharply, presumably due less to the rise of particle concentration between 2.6 and 4.6  $\mu\text{m}$  than to the rise below 1.4  $\mu\text{m}$ . Note that other possible causes of increased turbidity have not been ruled out; e.g., refractive index differences between particles and serum might have increased.

The effects of pasteurization upon skewness were opposite for the plant and laboratory processes. This contrast may reflect compositional differences that are due to: (a) variations in fruit origin and history, including length and type of storage, (b) alteration of the composition of the particle-serum system by processing procedures such as extraction and finishing, and (c) differences in the pasteurization technique.

In the laboratory the effects of evaporative concentration differed markedly from the effects of pasteurization. Particle concentration dropped sharply, large particles were preferentially lost, and there was no evidence of a gain in particle count anywhere in the size range examined; cf. Figure 4B. The heaviest loss centered around an effective diameter of 9  $\mu\text{m}$ , and the greatest resistance to loss was in the range of about 1–2  $\mu\text{m}$ . Comparison of Figures 3D and 4B shows the striking contrast between the effects of concentration in the laboratory vs. the plant.

Whether processing effects were examined in terms of changes in the skewness of size distributions or in terms of difference distributions, it is clear that they had complex origins. The magnitude of the changes in particle properties is emphasized by the experimentally independent quantity, scattering strength; variation was fivefold.

The processing stages can be tentatively ranked in terms of their potency in restructuring particle size distributions by using the mean deviation results of Table III. The tentativeness of this ranking rests on the lack of information about such processes as particle association and about other kinds of growth that may have occurred.

The data in Table II show that processing produced rather consistent trends in particle concentration, modal diameter, and distribution width. Evidently, the character of these trends was largely determined by the decreases that occurred in the concentration of large particles. The generally upward-concave appearance of the curves in Figure 3, as compared with those in Figure 4, may be due to comminution of rag and pulp during plant extraction and finishing. Such particles would be expected to be relatively immune to shear disruption as compared with cell organelles or similar particles. The appearance of new, large particles at the plant concentration stage, however, may have little to do with the presumed presence of rag and pulp particles; such phenomena as particle coagulation or the crystallization of previously dissolved substances may be responsible.

We believe that the understanding of juice particulate systems can be extended by further application of methods similar to those reported here.

#### ACKNOWLEDGMENT

We thank Clarence Taylor for providing the commercial samples. We are grateful for reviews provided by Vincent Maier, Carl Vandercook, and Henry Yokoyama. Fred Payne assisted in the measurement of particle size.

#### LITERATURE CITED

- Carnahan, B., Luther, H. A., Wilkes, J. O., "Applied Numerical Methods", Wiley, New York, N.Y., 1969.
- Hahn, G. J., Shapiro, S. S., "Statistical Models in Engineering", Wiley, New York, N.Y., 1967.
- Hildebrand, F. B., "Introduction to Numerical Analysis", McGraw-Hill, New York, N.Y., 1974.
- Venolia, W., Peak, S., Payne, F., *J. Agric. Food Chem.* **22**(1), 133 (1974).

Received for review November 14, 1975. Accepted March 25, 1976. Reference to a product name or company does not imply endorsement of that product or company by the U.S. Department of Agriculture to the exclusion of others that may be suitable.